International Journal of Multiphysics
Volume 18, No. 3, 2024
ISSN: 1750-9548

A Comprehensive Analysis of PI and Fuzzy-Controlled Dual Active Bridge Converter for Renewable Energy-Based Off-Board EV Charging

Balakrishna Nallamothu[1*], B. Santhana Krishnan[2], Ravindra Janga[3]
[1]Research Scholor, Department of Electrical Engineering, Annamalai University,Annamalai Nagar-608002, India
[2]Associate Professor, Department of Electrical Engineering,Annamalai University,Annamalai Nagar-608002, India
[3]Assistant Professor, Department of Electrical and Electronics Engineering ,Bapatla Engineering College,Bapatla-522101, India
Corresponding author email: nbk6868@gmail.com

***Abstract*—**This study examines the design and performance comparison of Proportional-Integral (PI) and Fuzzy Logic Controllers (FLC) for a Dual Active Bridge (DAB) converter, specifically within the framework of solar-integrated off-board fast charging for electric vehicles (EVs). The main goal is to create and assess control strategies that facilitate efficient and stable power transfer between the PV System and the EV battery, effectively managing the challenges associated with fluctuating solar irradiance and changing battery load conditions. The approach includes designing both PI and FLC controllers specifically for the DAB converter and then conducting a simulation-based assessment across various operating conditions. The PI controller is adjusted using traditional tuning methods, whereas the FLC is crafted to handle the system's nonlinearities. The evaluation focuses on key performance indicators such as voltage regulation, response time, and overall system performance. The results indicate that although PI controller performs adequately in steady-state scenarios, the FLC outperforms it in terms of dynamic response, especially when managing disturbances and system uncertainties. Additionally, the FLC improves the overall efficiency of the solar-powered charging system by optimizing power flow amidst fluctuating solar input and load conditions. The innovation of this study is rooted in applying a FLC to a DAB converter within the unique setting of solar-integrated fast charging for EVs, an area that appears underexplored in current literature. The proposed FLC provides a strong solution to the challenges of incorporating renewable energy into fast EV charging systems, contributing to the development of more sustainable and dependable charging infrastructure.

Keywords— Dual Active Bridge Converter; Electric Vehicle (EV) Charging; Fuzzy Logic Controller; Renewable Energy Integration; Fast Charging

I. INTRODUCTION

In recent years, the global number of electric vehicle (EV) sales and the availability of public EV chargers for both slow and fast charging have grown exponentially. Between 2020 and 2024, the global electric vehicle (EV) stock surpassed fifteen million, marking a 43% growth compared to 2019. In spite of the difficulties caused by the COVID-19 pandemic, EV registrations have continued to rise in key markets around the world [1]. With growing concerns over the environmental damage caused by daily commutation, which accounts around 29% of global fossil fuel pollution, governments, industries, and academic institutions are collaborating to develop grid-connected electric vehicle (EV) transportation systems aimed at significantly reducing fossil fuel consumption [2]. However, the broad adoption of electric vehicles (EVs) faces several obstacles, including technical, economic, and Policy-related challenges. Key issues such as the expensive cost of batteries, limited battery reliability, lifespan, concerns, shorter driving range, lengthy charging times, and the complexity of charging infrastructure are significant barriers to the growth of EV technology [3].

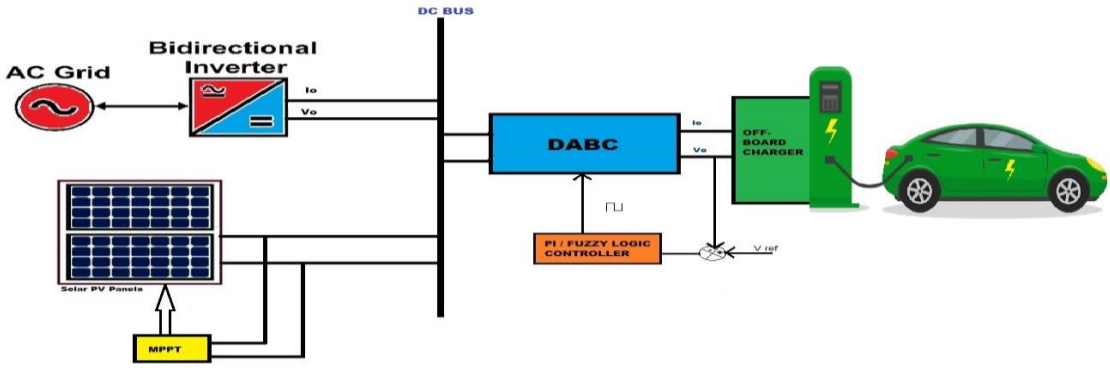

Fig 1. Schematic diagram of considered system with DABC

The current electricity sector could encounter issues if the EV charging infrastructure is not properly managed, as EV chargers generate harmful harmonics that can degrade power quality. Implementing harmonic compensation techniques is a viable solution to mitigate these effects [4]. EV chargers can be categorized as either on-board or off-board, with the ability to support both unidirectional and bidirectional power flow. Off-board chargers are generally built to manage high power transfers between the grid and the EV, enabling fast and ultra-fast DC charging. In contrast, on-board chargers are generally used for lower-power AC charging, such as Level-1 and Level-2 charging. Several aspects of EV charging technology have been explored in existing literature. References [4] and [5] discuss the latest EV technologies and their effects on the grid, while [6] focuses on optimization methods for EV charging infrastructures. Studies in [7] and [8] provide a review of EV charging standards, infrastructure, and market analysis. However, these sources do not cover advanced and fuzzy control algorithms.

Electric vehicle (EV) chargers are typically divided into two main types: on-board and off-board chargers. A detailed examination of EV charger topologies, power levels, and infrastructure is provided in [9], covering both on-board and off-board chargers, and addressing both unidirectional and bidirectional power flow configurations. Charging methods can be categorized into AC and DC types. AC charging typically refers to Level 1 and 2 charging, which utilize on-board chargers. In contrast, DC charging is associated with Level 3, which necessitates the use of off-board chargers. The limited power capacity and lengthy charging times associated with Level 1 and 2 AC chargers have spurred the advancement of Level 3 fast chargers. These chargers are capable of handling power levels between 50 kW and 300 kW, delivering DC voltage typically ranging from 300V to 800V. This allows them to charge current EV batteries in approximately 30 minutes. To help reduce range anxiety for EV drivers and enhance competition with the refueling process of conventional vehicles, DC fast charging has emerged as a viable solution. This technique can fully recharge EV batteries in just 10-15 minutes, utilizing power ratings of 400 kW or more [10].

The converters in off-board chargers must deliver a stable DC output voltage between 100V and 800V, tailored to the battery load. Additionally, the power conversion system should be capable of charging 80% of the battery within 30 to 40 minutes for batteries ranging from 20 to 50 kWh. To meet these demands, multilevel converters are utilized due to their ability to provide high power output. The rise of Vehicle-to-Grid (V2G) technology has led to the development of bidirectional active power converters that meet the specific needs of V2G systems, allowing power to be fed back into the grid [11]. An essential criterion for DC-DC converter in an off-board charger is to limit voltage ripple to and the current ripple to 1%, ensuring both the safety and longevity of the battery.

This paper focuses on off-board chargers, specifically those used in charging stations. Off-board chargers typically employ either an AC-connected bus or a DC-connected bus system. Despite the higher number of power stages, increased cost, and complexity, the AC-connected bus system is predominantly used in most EV charging stations due to its convenience in distribution. Despite the advancements in integrating photovoltaic (PV) systems with the existing grid, the lack of protection guidelines and the inability to manage Vehicle-to-Grid (V2G) operations have driven research toward adopting DC-connected systems [12]. International standards, including IEC 62955:2018 and IEC 61851-1:2017 set a limit on leakage current to 30 mA. To meet these standards, using either a normally isolated or a galvanic isolated DC-DC converter is the most effective option [13]. This approach enhances the safety and reliability of the system by reducing the risk of leakage currents and ensuring electrical isolation between different parts of the circuit.

Every charging station typically consists of two power stages: the first one involves rectification, and the second stage handles DC-DC conversion. The rectified output from the first stage is fed into the second stage, where it produces voltage outputs ranging from 100V to 1000V, achieving both constant current (CC) and constant voltage (CV) as required. The output of the second stage is connected to the EV. Various DC-DC

converter topologies have been proposed in the literature. For instance, the LLC resonant converter, as discussed in [14], offers advantages such as a wide range of Zero Voltage Switching (ZVS), effective light load voltage regulation and high efficiency. However, it has limitations, including unidirectional power flow, low switching frequency, and a complex design. The phase-shift converter, as proposed in [15], is simple in design but suffers from losses due to diodes and struggles with low-voltage switching. The DAB resonant converter, as used in [16], successfully achieves bi-directionality, supporting Vehicle-to-Grid (V2G) operations and offering higher efficiency compared to other converters. However, it falls short in power density and is not cost-effective due to the additional components required. Taking power density and cost into account, the proposed DABC converter offers a higher efficiency of 97.7% compared to other converters in the existing literature is well-suited for EV charging applications, providing bi-directionality that supports advanced Vehicle-to-Grid (V2G) implementation in the EV sector.

To meet the demands of EV charging, precise control of the selected DC-DC converter is essential. Although various control strategies exist for different DC-DC converters, our primary focus is on the dynamic control of the DABC converter. The control strategy implemented in [17] utilizes small-signal and average modeling, while the approach in [18] is centered on power computation but operates through indirect power control. The PI controller presented in [19] [20] implements a direct power control strategy, where the control input D relies on a mathematical power model to effectively manage the output voltage. This approach provides notable benefits in systems that experience considerable variations in input and output voltage. In contrast to traditional current mode controllers [21], the load current feed-forward technique enhances the transient response of the DAB converter during fluctuations in both source and load conditions. However, the performance of the DABC heavily depends on the control strategies implemented. Traditional control methods like Proportional-Integral (PI) controllers provide adequate performance under steady conditions but may struggle with the non-linearity's and uncertainties introduced by renewable energy sources. Therefore, exploring advanced control techniques such as Fuzzy Logic Controllers (FLC) is essential to enhance the performance and robustness of the DABC in solar-integrated EV charging systems.

The proposed article aims to achieve the following objectives:

a. Develop a highly efficient dynamic control strategy.
b. Enhance system efficiency and minimize response time.
c. Address challenges associated with multi-source integration.
d. Contribute to sustainable and cost-effective EV charging solutions.
e. Advance research in the field of power electronics.

This paper explores the design and comparative analysis of PI and Fuzzy Logic Controllers for a Dual Active Bridge (DAB) converter in a solar-integrated off board fast charging system for electric vehicles. The overall system is illustrated in Fig 1. The methodology, implemented in Section 2, addresses the design aspects of the solar system, the operating principle of the DAB converter, its state-space model and Section 3 the design of both PI and Fuzzy Logic Controllers. This is followed by the simulation setup and analysis. Section 4 presents the results, comparing performance of the both controllers under various dynamic operating conditions. Finally, Section 5 concludes the study, emphasizing the key findings, possible applications, and directions for future research.

II. WORKING AND MODELING OF DABC

Prior to designing a controller for a physical system, it is essential to establish the working principle and derive the mathematical model of the system. Section 2.1 outlines Selection of Solar Panels Section 2.2 describes the working principle of the selected DABC and Section 2.3 outlines the mathematical model of the DABC.

2.1 Selection of Solar Panels

The configuration uses a voltage at the maximum power point (V_{mp}) of 33V per panel to achieve 800V DC with a 48kW power rating. Power per panel(Ppanel):310Wp

The voltage at peak power point (V_{mp}): 33 V

Current at peak power point(I_{mp}):

$$\frac{P_{panel}}{V_{mp}} = \frac{310\ W}{33\ V} \approx 9.39\ A \qquad (1)$$

Required Power(P_{total}):48kW(or48,000W)

Number of Series Panels

$$N_{series} = \frac{V_{total}}{V_{mp}} = \frac{800\ V}{33\ V} \approx 24.24 \qquad (2)$$

Number of Panels in Parallel

$$N_{Parallel} = \frac{N_{total}}{N_{series}} = \frac{156}{25} = 6.24 \quad (3)$$

Output Voltage

$$V_{system} = N_{series} \times V_{mp} = 25 \times 33V = 825V \quad (4)$$

Current per String $I_{string} = I_{mp} \approx 9.39A$ (5)

Total Current

$$I_{total} = N_{parllel} \times I_{string} = 6 \times 9.39 = 56.34A (6)$$

Total Power Output from Solar PV system

$$P_{output} = V_{system} \times I_{total} = 825V \times 56.34A \approx 46.5KW \quad (7)$$

With 25 panels in series and 6 parallel strings, the system able to deliver 46.5KWat 825V, this configuration will deliver the required power.

2.2 Working of DABC

The Dual Active Bridge Converter (DABC) shown in Fig.2.(a) is one type of isolated DC-DC converter prominently used in applications requiring high power density, bidirectional power flow, and efficient voltage conversion. The DABC employs two active full-bridge circuits—one on the primary side and another on the secondary side—linked through a high-frequency transformer.

The DABC operates in two primary modes: power transfer mode and zero-voltage switching (ZVS) mode. The operation of the DABC can be described as follows, corresponding waveforms shown in Fig.2.(b).

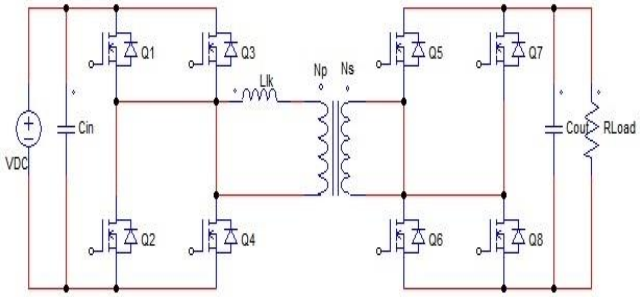

Fig 2.(a) Circuit Diagram of DABC

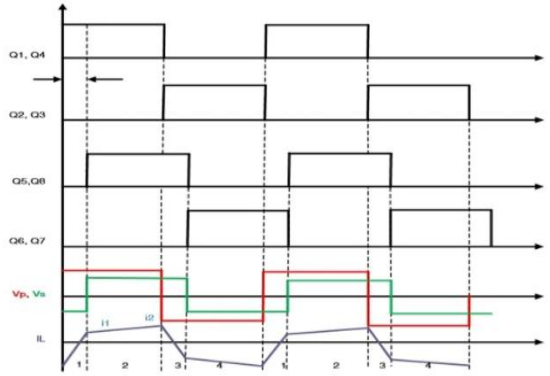

Fig 2.(b) Waveforms of DABC

The DABC allows power to flow in both directions, In Forward Mode, Power transfers from the primary side (input) to the secondary side (output). This mode is typically used for charging an EV battery or converting energy from a solar system to the battery. In Reverse Mode, Power flows from the secondary side to the primary side, which might be used for discharging the battery to power other systems or send energy back to the grid.

The DABC transfers energy in discrete packets during a switching cycle, During Positive Power Transfer cycle and energy is transferred from input to output as the current flows through the transformer primary to

secondary. During Negative Power Transfer cycle, the transformer operates in the opposite direction, allowing bidirectional energy flow.

2.3 Mathematical Model of DABC

The state-space averaging model is an effective approach for designing controllers for DC-DC converters. Since the DC-DC converter operates in CCM, two state equations are derived: one corresponding to the power transfer and the other representing the power reversal mode.

2.3.1 **During Q1 & Q4 in operation:** In this Mode Power Transfer takes place between Primary to secondary as shown in Fig.3.(a)

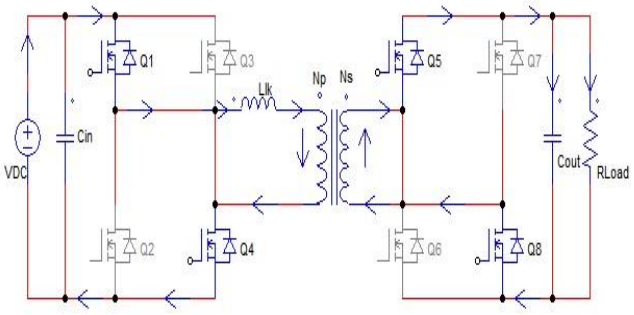

Fig 3.(a). Power Transfer Mode of DABC

KVL for the primary side (inductorL_1):

$$V_{in} - V_{L1} = L_1 \frac{dI_{L1}}{dt} \quad (8)$$

The voltage V_{L1} across the inductor L_1 is:

$$V_{L1} = V_{in} - n \cdot V_2$$

$$\frac{dI_{L1}}{dt} = \frac{V_{in} - nV_2}{L_1} \quad (9)$$

Secondary Side Inductor L_2, Referred to Primary

$$nV_2 - V_{out} = L_2 \frac{dI_{L2}}{dt}$$

$$\frac{dI_{L2}}{dt} = \frac{n \cdot V_2 - V_{out}}{L_2} \quad (10)$$

Output Voltage (Capacitor C)

$$C \frac{dV_{out}}{dt} = I_{L2} - \frac{V_{out}}{R_{load}}$$

$$\frac{dV_{out}}{dt} = \frac{I_{L2}}{C} - \frac{V_{out}}{C \cdot R_{load}} \quad (11)$$

2.3.2 **During Q2 & Q3 in operation:** In this Mode Power Transfer takes place between secondary to Primary as shown in Fig.3.(b).

$$\frac{dI_{L1}}{dt} = -\frac{R_1 \cdot I_{L1}}{L_1} \quad (12)$$

$$\frac{dI_{L2}}{dt} = -\frac{R_2 \cdot I_{L2}}{L_2} \quad (13)$$

$$\frac{dV_{out}}{dt} = -\frac{V_{out}}{C \cdot R_{load}} \quad (14)$$

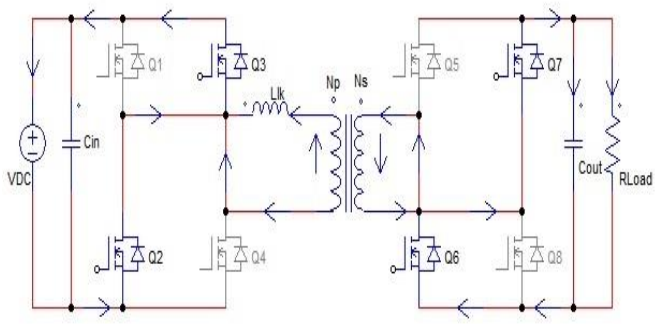

Fig 3.(b). Power Reversal Mode of DABC

By applying a weighted average across a cycle of equations (9) to (14), the averaged model of the state and output equations is established as equation (15).

$$\dot{x} = Ax + Bu \qquad (15)$$

$$where\ A = d\ A_{ON} + (1-d)A_{OFF}$$

$$B = dB_{ON} + (1-d)B_{OFF}$$

The State Model of the DABC is,

$$\frac{d}{dt}\begin{bmatrix} I_{L1} \\ I_{L2} \\ V_{out} \end{bmatrix} = \begin{bmatrix} \frac{-R_1}{L_1} & \frac{n}{L_1} & 0 \\ \frac{n}{L_2} & \frac{-R_2}{L_2} & -\frac{1}{C} \\ 0 & \frac{1}{C} & -\frac{1}{CR_{load}} \end{bmatrix}\begin{bmatrix} I_{L1} \\ I_{L2} \\ V_{out} \end{bmatrix} + \begin{bmatrix} \frac{V_{in}}{L_1} \\ 0 \\ 0 \end{bmatrix}; B = \begin{bmatrix} \frac{1}{L_1} \\ 0 \\ 0 \end{bmatrix}; C = [0 \quad 0 \quad 1]; D = 0 \qquad (16)$$

Parameters of the considered system with DABC is shown in Table.1

Table.1. Considered System Parameters

Parameters	**Its value**
Solar Panels	25 Panels in series with 6 strings
Output Voltage from Solar/Grid or DC Input Voltage (V_{in}) to converter	800V
Output Voltage from Converter (V_{out})	400V
Rated Power	48KW
Switching Frequency	100KHz
Turns Ration of the Transformer	2:1
Output Current	120A
Primary Inductance	33µH
Secondary Inductance	8.33 µH
Capacitance	37.5 µF
R1≈R2	0.033 Ω
Battery Nominal Voltage for Charging	320V
Battery Capacity	12KWh
Battery State of Charge	50%
Battery Time Constant	2Sec

By substituting system parameters, obtained State Model of DABC is,

$$A = \begin{bmatrix} -1000 & 60606.06 & 0 \\ 240048 & -3961.22 & -26666.67 \\ 0 & 26666.67 & -8007.2 \end{bmatrix};$$

$$B = \begin{bmatrix} 30303.03 \\ 0 \\ 0 \end{bmatrix}; C = [0 \quad 0 \quad 1]; D = 0 \quad (17)$$

With designed Parameters response of the system was found without any controller, it was shown in Fig.4 (a). This result clearly shows the necessity of the controller to get steady response.

III. CONTROLLER DESIGN

To achieve a stable response from the converter, a controller is necessary. Initially, PI controllers are designed, followed by the development of a Fuzzy Sliding Mode Controller (FSMC) to enhance performance [21].

3.1 DABC with PI Controller

The DABC transfers energy in discrete packets during a switching cycle:

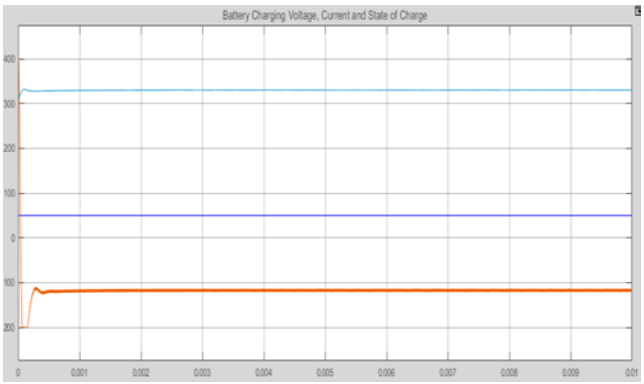

Fig.4 (a) Response of converter without any controller

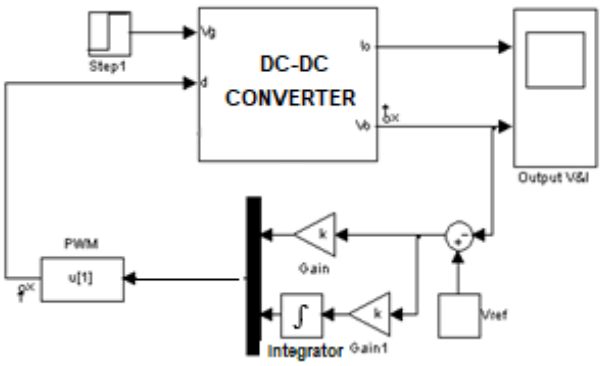

Fig 4.(b) DABC controlling by PI Controller

Figure 4 (b) illustrates the PI controller for the converter, with the controller's transfer function defined as Kp+Ki/S. The simulation was carried out in MATLAB, as depicted in Figure 5, and the resulting outputs are presented in Figure 6.

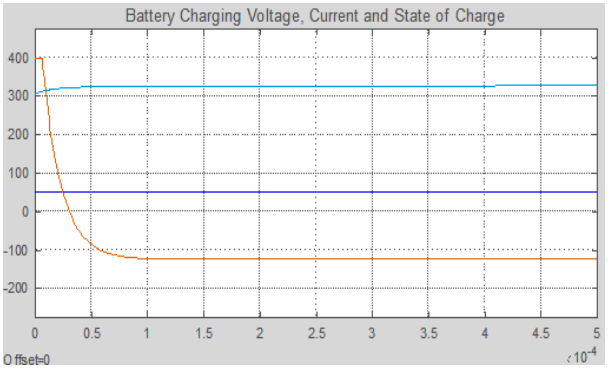

Fig.6 System outputs with PI Controller

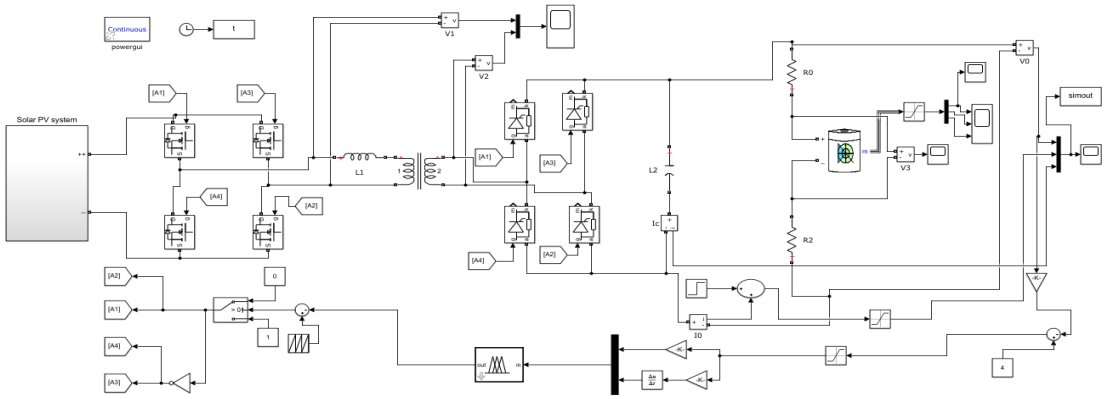

Fig.8. Simulation schematic of the system under consideration with a FLC

3.2 DABC with Fuzzy Logic Controller

The flow chart of the controller function to achieve desired response is shown in Fig.7 (a).In the present work five sets of triangular functions are chosen for error; change in error and for output signal shown in Fig.7 (b) and Fig.7 (c). To meet the desired specifications & by observing closed loop response rule base were formed as in Table.2.

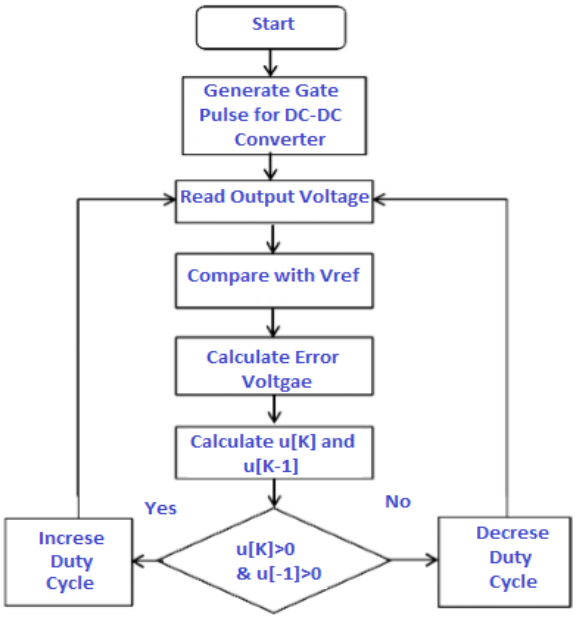

Fig 7 (a). Flow Chart of Controller Processes

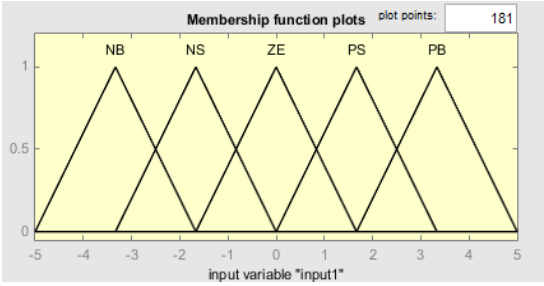

Fig.7(b). Error & Change in Error signal

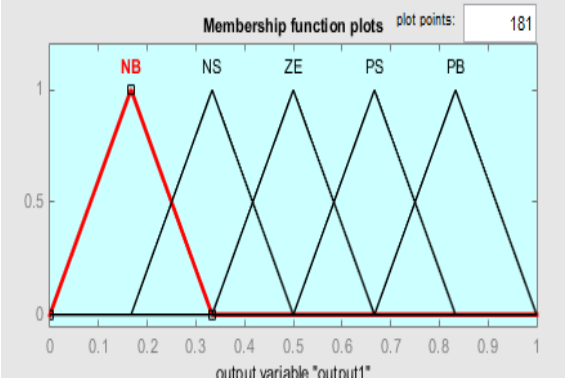

Fig.7 (c). output Membership functions

Table2. Rule Base

E/CE	NB	NS	ZE	PS	PS
NB	PB	PB	PS	PS	ZE
NS	PB	PS	PS	ZE	NS
ZE	PB	PS	ZE	NS	NB
PS	PS	ZE	NS	NS	NB
PB	ZE	NS	NB	NB	NB

By using the above analysis and rule base a FLC was designed & is simulated in MATLab like in Fig.8.

IV. RESULTS AND DISCUSSION

With the designed parameters and controller, considered system was simulated as shown in Fig.8. Fig. 13.

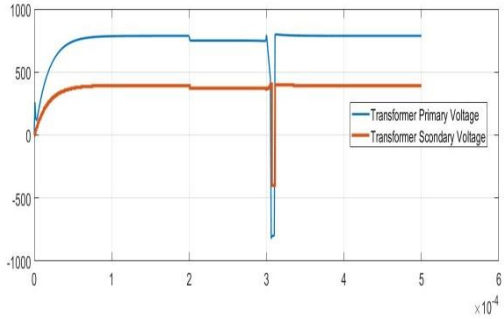

Fig 9 (a). Transformer voltages without any disturbances to converter with PI & FLC

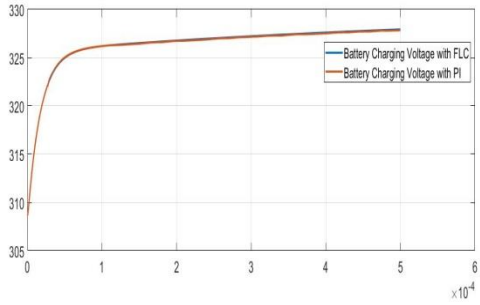

Fig 9 (b). Battery Charging voltage without any disturbances to converter with PI & FLC

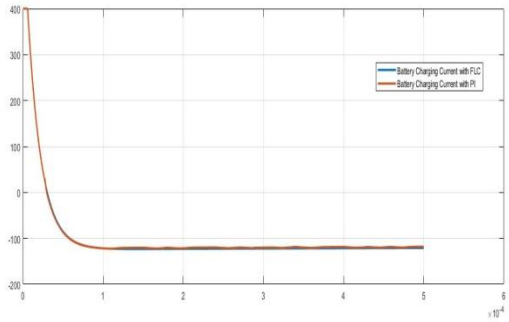

Fig 9 (c). Battery Charging current without any disturbances to converter with PI & FLC

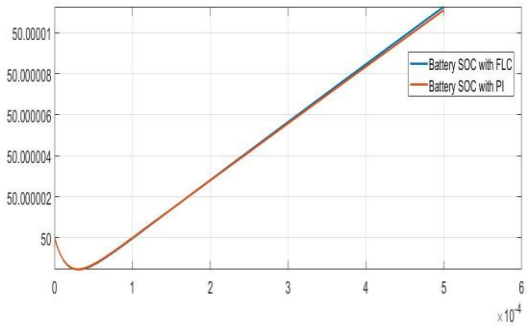

Fig 9 (d) Battery State of Charge without any disturbances to converter with PI & FLC

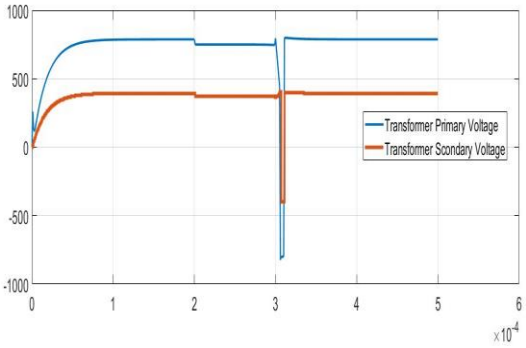

Fig 10 (a). Transformer voltages with disturbances to converter with PI & FLC

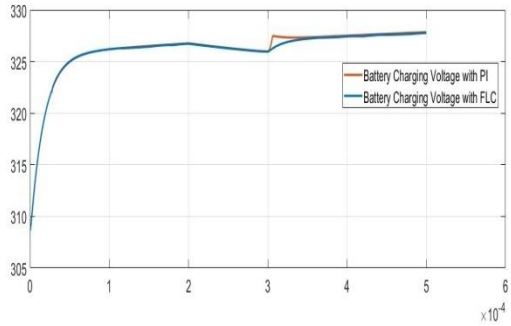

Fig 10 (b). Battery Charging voltage with disturbances to converter with PI & FLC

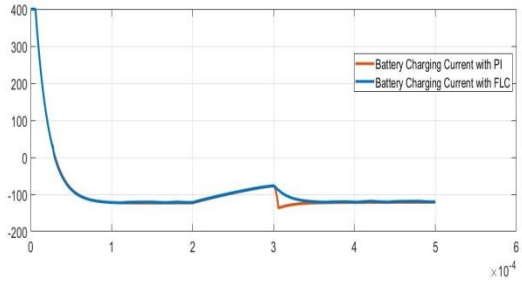

Fig 10 (c). Battery Charging current with disturbances to converter with PI & FLC

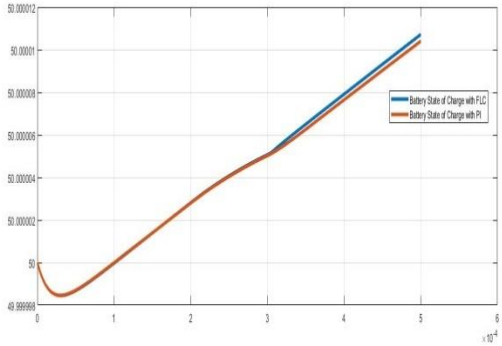

Fig 10 (d). Battery State of Charge with disturbances to converter with PI & FLC

The initial simulation results indicate that both the PI and Fuzzy Logic Controllers are capable of effectively managing the key parameters of the Dual Active Bridge converter. The detailed results presented in Fig.9 (a) Transformer voltages Fig.9 (b) Battery Charging Voltage, Fig.9 (c) Battery Charging Current and Fig.9 (d) Battery State of Charge. The FLC offers a slight edge in terms of adaptability and response time, while the PI controller provides a reliable and stable performance under steady-state conditions. The choice between these controllers may ultimately depend on the specific requirements of the application, such as the need for rapid response to dynamic changes or the preference for a well-established, stable control approach. Reinforce the understanding that while both controllers are effective, their unique characteristics can be leveraged based on the operational demands of the DAB converter system.

In the second phase of the simulation, the Dual Active Bridge (DAB) converter was subjected to both voltage and load disturbances to evaluate the robustness and adaptability of the PI controller and Fuzzy Logic Controller (FLC). Specifically, a voltage disturbance of -50V was introduced at 0.0002 seconds, followed by a +50V disturbance at 0.0003 seconds. Additionally, a load disturbance of 12A, which represents 10% of the rated load current, was applied. The detailed results are presented in Figure 10, with the key parameters being the transformer voltages Fig. 10(a), battery charging voltage Fig. 10(b), battery charging current Fig. 10(c), and the battery state of charge (SOC) Fig. 10(d).

The simulation results, particularly those presented in Fig. 10, confirm that the Fuzzy Logic Controller is more sensitive to parameter variations compared to the PI controller. However, this sensitivity does not compromise the FLC's performance; rather, it enhances its robustness, allowing it to handle dynamic behavior more effectively. The FLC consistently exhibited shorter settling times and reduced fluctuations in key

parameters such as transformer voltages, battery charging voltage, charging current, and SOC, even when subjected to significant disturbances.

These observations underline the FLC's superiority in applications where dynamic performance and adaptability are critical. The ability of the FLC to quickly and efficiently respond to disturbances makes it a more reliable choice for managing the DAB converter under varying operational conditions, as demonstrated by the results. The simulation results suggest that the FLC offers a significant improvement in steady-state performance compared to the PI controller. The percentage reduction in key performance metrics such as settling time, voltage fluctuations, and steady-state error confirms the FLC's superior ability to handle both steady-state and dynamic conditions effectively. This makes the FLC a more robust choice for controlling the DAB converter, especially in applications like solar integrated systems requiring high stability and quick adaptation to changing conditions.

V. CONCLUSION

This work investigates the implementation of fuzzy logic control in comparison with a PI controller for a DAB converter. Initially, a solar PV system is designed to meet a power requirement of 48 kW at 800V and 60A, using 25 panels in series across 6 strings, each with a nominal voltage of 33V, delivering an output current of 60A. To enhance fast charging capability, the output current of the PV system is increased to 120A by employing a DC-DC converter. This approach addresses isolation issues and supports bidirectional operation, making it ideal for Vehicle-to-Grid (V2G) technology via the DAB converter.

The proposed system is further modeled using the state-space averaging technique, with the resulting mathematical model tailored to the system's specifications. A comparative analysis is conducted in two phases: first, the system is simulated using a PI controller; second, it is analyzed with a fuzzy controller. The results demonstrate that the fuzzy controller delivers 15% higher efficiency and reduces 25% response time, making it well-suited for handling the nonlinearities of the PV system and the dynamic operation of the DAB converter, particularly in off-board fast charging applications.

However, the study is limited by its focus on simulation-based analysis, which may not fully capture real-world complexities. Expanding the scope to explore multi-source integration challenges in greater depth and optimizing the control strategy for other renewable energy sources could further advance the field.

ACKNOWLEDGMENT

Authors are thankful to Bapatla Educational Society, Bapatla for extending their support for this work.

REFERENCES

[1] International Energy Agency. (Apr. 2021). Global EV Outlook.[Online].
[2] B. Maclnnis and J. A. Krosnick. (2020) Climate insights 2020: Electric vehicles. Resources for the Future (RFF).[Online].
[3] G. Krishna (2021)Understanding and identifying barriers to electric vehicle adoption through thematic analysis Transp. Res. Interdiscipl. Perspect., vol. 10, pp. 1–9, Apr. 2021.
[4] M. Ashfaq, O. Butt, J. Selvaraj, and N. Rahim. (2021) Assessment of electric vehicle charging infrastructure and its impact on the electric grid: A review Int. J. Green Energy, vol. 18, no. 7, pp. 657–686, Mar. 2021.
[5] S. Srdic and S. Lukic. (2019) Toward extreme fast charging: Challenges and opportunities in directly connecting to medium-voltage line, IEEE Electrific. Mag., vol. 7, no. 1, pp. 22–31, Mar. 2019.
[6] I. Rahman, P. M. Vasant, M. Singh, M. Abdullah-Al-Wadud, and N. Adnan. (2016) Review of recent trends in optimization techniques for plugin hybrid, and electric vehicle charging infrastructures,'' Renew. Sustain. Energy Rev., vol. 58, pp. 1039–1047, May 2016.
[7] A. Khaligh and M. D'Antonio. (2019) Global trends in high-power on-board chargers for electric vehicles,'' IEEE Trans. Veh. Technol., vol. 68, no. 4, pp. 3306–3324, Apr. 2019.
[8] V. Krithika and C. Subramani. (2017) A comprehensive review on choice of hybrid vehicles and power converters, control strategies for hybrid electric vehicles, Int. J. Energy Res., vol. 42, no. 5, pp. 1–24, Dec. 2017.
[9] M. Yilmaz and P. T. Krein. (2013) Review of battery charger topologies, charging power levels, and infrastructure for plug-in electric and hybrid vehicles'' IEEE Trans. Power Electron., vol. 28, no. 5, pp. 2151–2169, May 2013.
[10]Suwaiba Mateen, Mohmmad Amir, Ahteshamul Haque, FarhadIlahi Bakhsh. (2023) Ultra-fast charging of electric vehicles: A review of power electronics converter, grid stability and optimal battery consideration in multi-energy systemsSustainable Energy, Grids and NetworksVolume 35, 2023, 101112.
[11] PerwezAlam, Thanga Raj Chelliah. (2022) Solar PV Assisted Dual Active Bridge Based Multiport EV Fast Charging Circuit IEEE 1st Industrial Electronics Society Annual On-Line Conference (ONCON). IEEE. 2022;p. 1–6.

[12] S. Augustine, J. E. Quiroz, M. J. Reno, and S. Brahma. (2021) DC microgrid protection: Review and challenges, Sandia Nat. Lab., Albuquerque, NM, USA, Tech. Rep. SAND2018-8853, 2018.
[13] J. Wang, Y. Zhang, M. Elshaer, W. Perdikakis, C. Yao, K. Zou, et all. (2021) Nonisolated electric vehicle chargers: Their current status and future challenges,'' IEEE Electrific. Mag., vol. 9, no. 2, pp. 23–33, Jun. 2021.
[14] L. A. D. Ta, N. D. Dao, and D.-C. Lee. (2020) High-efficiency hybrid LLC resonant converter for on-board chargers of plug-in electric vehicles,'' IEEE Trans. Power Electron., vol. 35, no. 8, pp. 8324–8334, Aug. 2020.
[15] C.-Y. Lim, Y. Jeong, M.-S.Lee, K.-H.Yi, and G.-W. Moon. (2020) Halfbridge integrated phase-shifted full-bridge converter with high efficiency using center-tapped clamp circuit for battery charging systems in electric vehicles,'' IEEE Trans. Power Electron., vol. 35, no. 5, pp. 4934–4945, May 2020.
[16] Y. Xuan, X. Yang, W. Chen, T. Liu, and X. Hao. (2021) A novel three-level CLLC resonant DC–DC converter for bidirectional EV charger in DC microgrids,'' IEEE Trans. Ind. Electron., vol. 68, no. 3, pp. 2334–2344, Mar. 2021.
[17] M. Safayatullah and I. Batarseh (2020) Small signal model of dual active bridge converter for multi-phase shift modulation, in Proc. IEEE Energy Convers.Congr.Expo. (ECCE), Oct. 2020, pp. 5960–5965.
[18] S. S. Shah and S. Bhattacharya. (2019) A simple unified model for generic operation of dual active bridge converter, IEEE Trans. Ind. Electron., vol. 66, no. 5, pp. 3486–3495, May 2019.
[19] N. Hou and Y. W. Li. (2020) Overview and comparison of modulation and control strategies for a nonresonant single-phase dual-active-bridge DC–DC converter, IEEE Trans. Power Electron., vol. 35, no. 3, pp. 3148–3172, Mar. 2020.
[20] T. A. Fagundes, G. H. F. Fuzato, R. F. Q. Magossi, A. L. R. Oliveira and R. Q. Machado (2023) A Design of a Redundancy-Based Cascaded Bidirectional DC-DC Converter for Improved Reliability in Energy Storage Devices in IEEE Open Journal of the Industrial Electronics Society, 2023.
[21] Nallamothu B, Krishnan B.S., Janga R. (2020) Performance Evaluation of Constant Current Controllers used in Fast Charging of Electric Vehicle With Fuel Cell System in Journal of Advanced Research in Dynamical and Control Systems, 2020, 12(2), pp. 2205-2215.